



ISSN: 0067-2904

GIF: 0.851

Theoretical Study of Bonds length, Energetic and Vibration Frequencies for Construction Units of (6,0) ZigZag SWCNTs

Rehab Majed Kubba*, Khalida Abaid Samawi

Department of Chemistry, College of Science, University of Baghdad, Baghdad, Iraq.

Abstract

Density Functional Theory (DFT) calculation of the type (B3LYP) and 6-311G basis set level using Gaussian-03 program were carried out for equilibrium geometry of construction units of (6,0) linear ZigZag SWCNT (mono, Di, Tri and Tetra ring layers), to evaluate the geometrical structure (bond length), symmetries, physical properties and energetic such as standard heat of formation (ΔH_f^0), total energy ($E_{tot.}$), dipole moment (μ), Highest Occupied Molecular Orbital Energy (E_{HOMO}), Lowest Unoccupied Molecular Orbital Energy (E_{LUMO}), energy gap ($\Delta E_{HOMO-LUMO}$), the distribution of electron density (ρ) and vibration frequencies, all at their equilibrium geometries. Assignment of the vibration frequencies according to the group theory was done applying the Gauss View program. Comparison were done for the distribution of electron density, vibration frequencies with the studying the relationship of all the physical and electronic properties for ZigZag SWCNTs with its construction units.

Keywords: ZigZag SWCNTs, bonds length, energetic, vibrations frequencies.

دراسة نظرية لاطوال اواصر وطاقات وترددات اهتزاز وحدات بناء انبوب كربون نانو منفرد نوع (6,0) ZigZag

رحاب ماجد كبة* ، خالدة عبيد سماوي

كلية العلوم، قسم الكيمياء، جامعة بغداد، العراق

الخلاصة

تم استخدام حسابات ميكانيك الكم العائدة لنظرية دوال الكثافة DFT الأساسية وبأسلوب B3LYP ولعناصر قاعدة 6-311G وباستخدام برنامج Gaussian-03 في حساب الشكل الهندسي التوازني لوحدات بناء انبوب نانو كربوني خطي نوع zigzag (6,0) (احادي وثنائي وثلاثي ورباعي الطبقات الحلقية) بغرض تقييم الشكل الفراغي (أطوال التآصر) والتماثل وبعض الصفات الفيزيائية والطاقية كحرارة التكوين القياسية (ΔH_f^0) والطاقة الكلية ($E_{tot.}$) وعزم ثنائي القطب (μ) وطاقة اعلى مدار محجوز بالالكترونات (E_{HOMO})، وطاقة اوطاً مدار غير محجوز بالالكترونات (E_{LUMO})، والفرق الطافي بينهما ($\Delta E_{HOMO-LUMO}$)، وتوزيع الكثافة الالكترونية (ρ) مع حساب وتصنيف ترددات الاهتزاز تكافؤيا ونماتلbia وفق نظرية المجموعة من خلال برنامج العرض لكوس. وتم اجراء مقارنة لتوزيع الكثافة الالكترونية ولترددات الاهتزاز مع دراسة علاقة كل ذلك بالخواص الفيزيائية والالكترونية لوحدات بناء انبوب النانو الكربوني نوع zigzag.

*Email: Rehab_mmr_kb@yahoo.com

Introduction

Carbon nanotubes (CNTs) have attracted increasing attention since their discovery. Because of their striking structural and electronic properties such as small diameters, high aspect ratios, high mechanical strength, and high thermal and chemical stability, carbon nanotubes are excellent field emitters and are thus potentially useful in field-emitting flat panel displays [1].

CNTs have attracted much attention because of their outstanding physical and mechanical properties. High axial modulus and tensile strength [2,3], low weight, small size, low density, high stiffness [4] and excellent thermal [5] and electrical properties [6] have encouraged many scientists to work on the issue. During recent years, mechanical characterization of CNTs has been one of the top issues in mechanical and materials engineering. Some of the most widely investigated applications include conductive and high-strength nanotube/polymer composites, transparent electrodes, sensors and nanoelectromechanical devices, additives for batteries, field emission displays and radiation sources, semiconductor devices (e.g. transistors) and interconnects [7].

It is expected that the cost and availability of nanotubes of consistent quality will soon become more in line with the industrial needs, and consequently the pace of development will greatly accelerate. The electronic structure of the carbon nanotube fragment and, the physical and chemical properties of the cluster depend strongly on the cluster size and point-group symmetry. The symmetry properties of a given nanotube fragment are determined by the number of hexagons along the tube axis, N , being even or odd and the number of hexagons along the tube circumference, n , being even or odd. The four possible combinations of these numbers give two different kinds of point groups (D_{nh} and D_{nd}), which, in turn, determine the differences in the structure of molecular orbitals, obtained from quantum chemical calculations [8].

Single-wall nanotubes (SWNTs) which were first reported in 1993 [9,10]. The SWNT are characterized by strong covalent bonding, a unique one-dimensional structure and nanometer size which impart unusual properties to the nanotubes including exceptionally high tensile strength, high resilience, electronic properties ranging from metallic to semiconducting, high current carrying capacity, and high thermal conductivity.

A SWNT is formed by wrapping a single sheet of graphite (graphene). It is interesting to note that graphene, by itself, can be characterized as either a zero-gap semiconductor or a metal, since the density of states (DOS) is zero at the Fermi energy, and imparts those properties to a nanotube. It is also well known that the fundamental conducting properties of a graphene tubule depend on the nature of wrapping (chirality) and the diameter (typically, SWNTs have diameters in the range 0.4nm-2nm).

The vibration frequencies of CNTs have been employed in the determination of the Young's modulus of CNTs [2,11-13]. One of the promising applications is the CNT-based ultra sensitive sensor. CNTs, in particular single-walled CNTs (SWCNTs), are small in size with large surface, stable in harsh chemical environment [14] and can respond to the external mechanical deformation rapidly with high sensitivity. It is of great significance to gain a full understanding of the vibration properties of SWCNTs. Vibration is one of the fundamental mechanical behaviors of CNTs. When compared with the extensive investigations of buckling or tensile behaviors of CNTs under axial loadings [15-20] relatively fewer studies have been done to analyze the vibration behaviors of CNTs. Similar to the buckling analysis of CNTs, the vibration behaviors of CNTs have usually been explored by two common methods, i.e. continuum mechanics models and atomistic simulations. In continuum mechanics modeling, the CNTs are treated as continuum and homogeneous structures without considering their intrinsic atomic structures.

To study the dependency of the electronic structure of $(n,0)$ nanotube fragments on their size, we have considered fragments of the $(6,0)$ tube. The $(6,0)$ carbon tube seems to have the lowest experimentally realizable diameter. As shown previously [21,22], tubes with a smaller diameter are thermodynamically unstable.

We considered $(6,0)$ tube fragments of different length. The dangling bonds at the ends of the nanotube fragments were saturated by hydrogen atoms. The structural unit of the tube is the distorted carbon hexagon.

The point group symmetry of the $(6,0)$ nanotube fragment is determined by the number N of carbon hexagons along the tube axis. Nanotube fragments with odd (n) belong to the group D_{nh} , where as nanotube fragments with even (n) belong to the group D_{nd} .

In our research Gaussian 03 and MOPAC computational packages have been employed throughout this study to compute the geometrical structure (bond lengths) for (6,0) zigzag Single Wall Carbon Nanotubes (SWCNTs), as well as the energetic Parameters, (heat of formation (ΔH_f^0), highest occupied molecular orbital energy (E_{HOMO}), lowest unoccupied molecular orbital energy (E_{LUMO}), the energy gap ($\Delta E_{\text{HOMO-LUMO}}$), dipole moment (μ)---etc. Comparison were done for the distribution of electron density with the expense of vibration frequencies and study the relationship of all the physical and electronic properties for all construction units, benzene, naphthalene, anthracene and (Mono, Di, Tri and Tetra) ring layers.

Computational Details

All the quantum chemical calculations were performed with complete geometry optimizations using Gaussian-03 software package [23]. Geometry optimization were carried out by B3LYP functional at the 6-311G basis set and at the density functional theory (DFT) level. BLYP functional is obtained by adding gradient corrections to the LDA method specifically the exchange correction of Becke [24] and the correlation function of Lee et al. [25].

Results and Discussion

To study the vibration motions of such molecules, one has to define its geometric parameters, and has to distinguish between the axial CC (C-Ca) bonds and circumferential CC (C-Cc) bonds.

The four classifications of carbon nanotubes (Mono, Di, Tri and Tetra)-ring layers, determined by the same of the numbers circumferential rings and different number of layers. CNT, can also be described as single-walled nanotubes (SWNT), resembling by rolling a graphene sheet into a cylinder mathematically structures are uniquely defined by specifying the coordinates of the smallest folding vector (n,0), zigzag SWCNT molecule is composed of annulated number of member aromatic rings molecules.

Figure-1 shows the structures of the equilibrium geometries of (6,0) zigzag SWCNTs construction units (Mono, Di, Tri and Tetra) ring layers, with symmetry of (D_{6h}), (D_{6d}), (D_{6h}), and (D_{6d}) respectively calculated by using DFT (B3LYP/ 6-311G) method, with the repetitive sections of bonds and angles. Table 1 shows the calculated bond distances for repetitive sections of the construction units of zigzag SWCNTs.

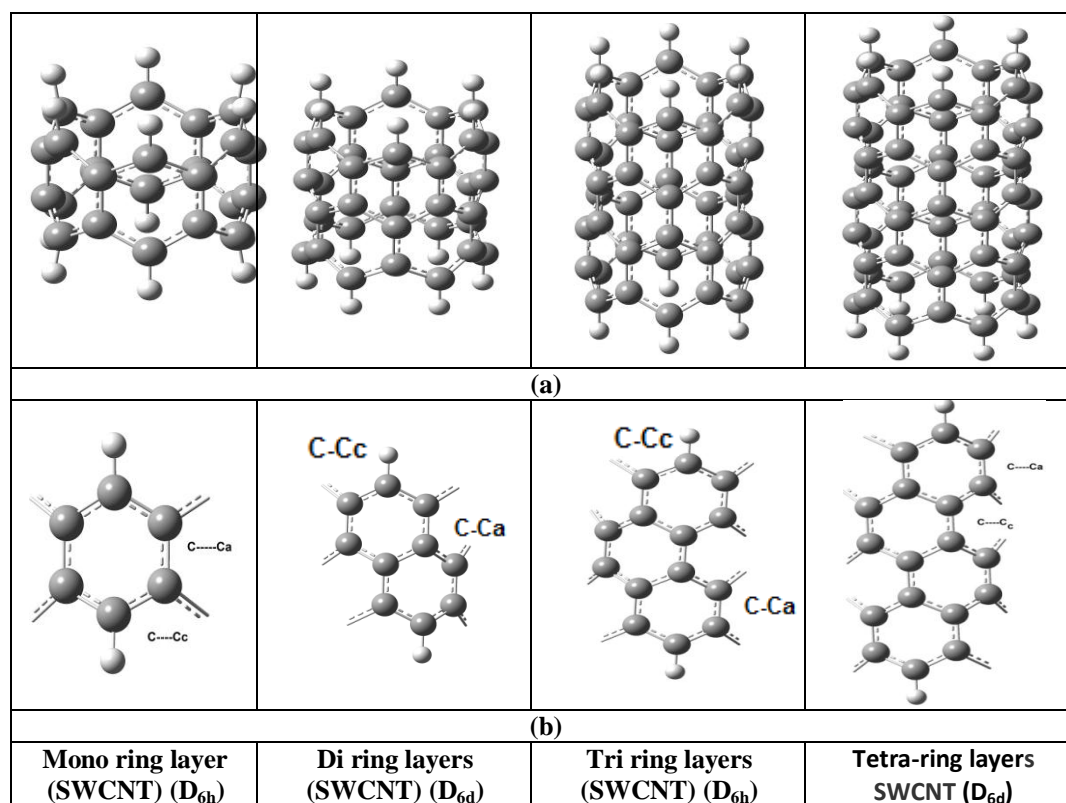


Figure 1- Construction units of (6,0) zigzag SWCNTs; (a) Equilibrium geometries of (Mono, Di, Tri and Tetra) ring layers, as calculated by DFT (6-311G/ B3LYP) level methods. (b) Repetitive sections of bonds for Mono, Di, Tri and Tetra) ring layers at their equilibrium geometries.

On doing correlations for bonds length of the construction units of (6,0) zigzag SWCNTs we noticed the following relations;

1- The bonds length of axial carbon-carbon (C-Ca) for coplanar molecule naphthalene and anthracene increases with increasing size of molecule and increasing from outer to inner direction. For SWCNTs of Tri and Tetra, the bonds length of axial carbon-carbon (C-Ca) decreases (decrease in force constant) with increasing the number of ring layers, and decrease in length from outer to mid layer of Di, Tri, and Tetra SWCNTs (increase in strength), Table-1, Figure-2.

2- The bonds length of circumferential carbon-carbon (C-Cc) for coplanar molecule naphthalene and anthracene decreases with increasing size of molecule and decreasing from outer to direction. For SWCNTs the reverse was found for (C-Cc) which increases (increase in force constant) with increasing the number of ring layers, and increase in length from outer layer to mid layer of Di, Tri, and Tetra SWCNTs (decrease in strength). These results agree well with literature [26] for all zigzag SWCNTs Table-1, Figure-2.

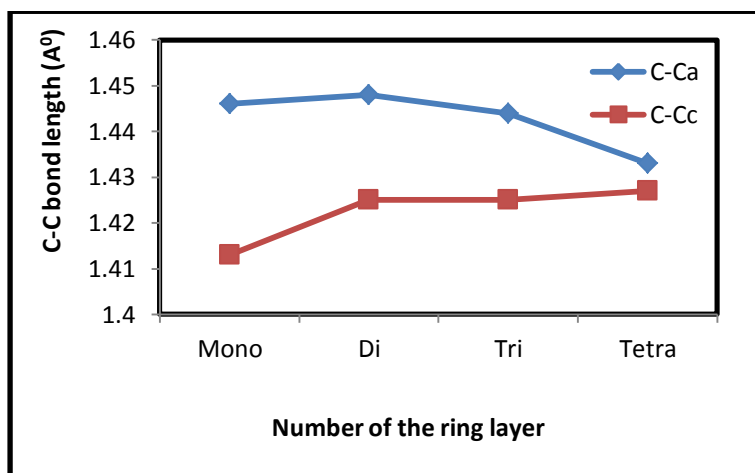


Figure 2- Correlation between the (C-Ca & C-Cc) bonds length and the number of ring layers.

3- The bonds length of C-H for Mono (1.095 Å) was shown to be longer than for Di, Tri, and Tetra (1.085 Å), Table-1.

4- The length of SWCNT increase with increasing the number of ring layers, Figure-3, Table-1.

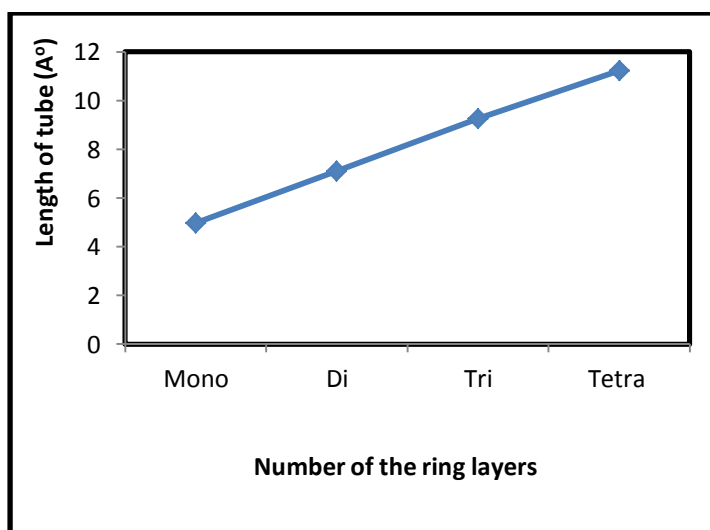


Figure 3- Correlation between length of SWCNT and the number of ring layers as calculated DFT method.

5- The diameter of SWCNT increase slightly with increasing the number of ring layers, Table-1.

Table-1- DFT calculated bond distances for construction units of (6,0) zigzag SWCNTs.

Zigzag ring layer SWCNT	Diameter (Å)	Length (Å)	Bond length (Å)		
			C...Ca	C-Cc	C—H
Benzene D _{6h}	-----	4.960	1.397	1.397	1.082
Naphthalene D _{2h}	-----	4.974	1.418 outer 1.436 inner	1.377 C=C 1.423 C--C	1.083 α 1.082 β
Anthracene D _{2h}	-----	4.977	1.428 outer 1.447 inner	1.370 C=C 1.432 C--C 1.402 C--C	1.083 α 1.082 β 1.084 (9,10)
Mono ring layer D _{6h}	4.816	4.972	1.446	1.413	1.095
Di-rings layer D _{6d}	4.823	7.114	1.448	1.425 outer 1.432 mid	1.083
Tri-ring layers D _{6h}	4.825	9.264	1.444 outer 1.436 mid	1.425 outer 1.434 mid	1.083
Tetra-ring layers D _{6d}	4.841	11.239	1.433 outer 1.420 mid	1.427 outer 1.444 mid 1.446 mid	1.083

C-Ca: axial bond.; C-Cc: circumferential bond.

For correlations of **physical properties** of (6,0) zigzag SWCNTs construction units, the following relations were noticed.

- 1- The standard heat of formation ΔH_f° was found to be increase with increasing number of ring layers for (6,0) Zigzag SWCNT as calculated by DFT Figure-4, Table-2.

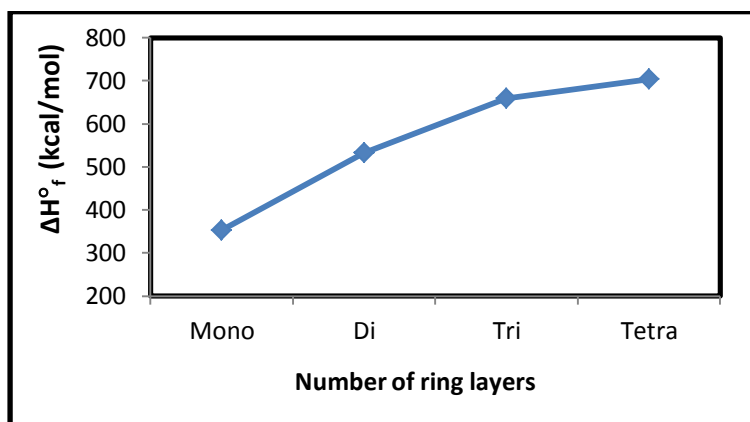


Figure 4- Correlation between the standard heat of formation ΔH_f° and the number of ring layers as calculated by DFT method.

- 2- The E_{HOMO} increases with increasing size of construction units of (6,0) zigzag SWCNT, Table-2. The higher HOMO energy corresponds to the more reactive molecule in the reactions with electrophiles.
- 3- The E_{LUMO} decreases with increasing size of construction units of (6,0) zigzag SWCNT, Table-2. lower LUMO energy is essential for molecular reactions with nucleophiles.
- 4- The $\Delta E_{\text{HOMO-LUMO}}$ decreases with increasing size of construction units of energy gap ($\Delta E = E_{\text{LUMO}} - E_{\text{HOMO}}$) Figure-5 and Table-2. $\Delta E_{\text{HOMO-LUMO}}$ is an important parameter as a function of reactivity of the inhibitor, SWCNTs, towards the adsorption on the metallic surface. As ΔE decreases the reactivity of the SWCNTs increases leading to increase in the inhibition efficiency (%IE) of the molecule. Lower values of the energy difference will render good inhibition efficiency, because the energy to remove an electron from the last occupied orbital will be low. Reportedly, excellent corrosion inhibitors are usually organic compounds which not only offer electrons to unoccupied orbital of the metal but also accept free electrons from the metal. A SWCNT with a low energy

gap is generally associated with the high chemical activity and low kinetic stability and is termed soft SWCNT [27].

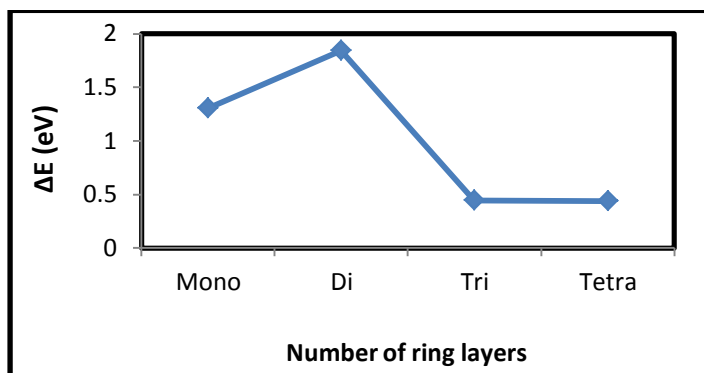


Figure 5- Correlation between the energy difference ($\Delta E_{\text{HOMO-LUMO}}$) and number of ring layers as calculated by DFT method.

Table 2- Some physical properties of the calculated construction units of (6,0) zigzag SWCNT at their equilibrium geometry.

Units cons. of zigzag SWCNT	m. wt. (g/ mol)	ΔH_f° (kcal/mol)	μ (Debye)	E_{HOMO} (eV)	E_{LUMO} (eV)	ΔE (eV) HOMO-LUMO
Benzen C_6H_6	78.000	21.954	0.000	-7.053	-0.191	6.862
Naphthalene $C_{10}H_8$	128.000	40.559	0.000	-6.105	-1.158	4.947
Anthracene $C_{10}H_8$	178.000	61.501	0.000	-5.501	-1.874	3.627
Mono-ring layer $C_{24}H_{12}$	300.359	353.370	0.000	-3.919	-2.611	1.307
Di-ring layers $C_{36}H_{12}$	444.491	532.942	0.000	-4.633	-2.793	1.840
Tri-ring layers $C_{48}H_{12}$	588.623	659.221	0.000	-4.000	-3.559	0.441
Tetra- ring layers $C_{60}H_{12}$	732.755	704.030	0.000	-3.822	-3.384	0.438

- 5- The distribution of electronic charge density for circumference carbon atom was found to increase with increasing number of odd (Mono and Tri) ring layers and decrease with increasing number of even (Di & Tetra) ring layers for (6,0) zigzag SWCNTs, Figure-6.

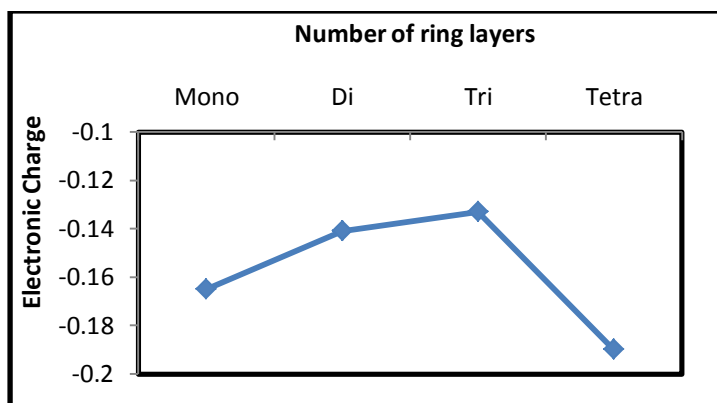


Figure 6- Correlation between the distribution of electronic charge (ρ) for outer circumference carbon atoms and the number of ring layers.

Similar to the carbon nanotubes [28-31], the charge densities are mainly concentrated at the circumferential carbon and hydrogen atoms of mono and multi-rings layer SWCNT, parallel with their physical properties for electrical conductivity.

The axial carbon atoms possess diminishing charges from outer to center direction. The H atoms are positively charged, whereas the C atoms are of the negative charge for (Mono, Di, Tri and Tetra) ring layers of (6,0) Zigzag SWCNT as calculated by DFT (6-311G/ B3LYP), Figure-7.

The physical and chemical properties of the SWCNT depend strongly on the size and point-group symmetry. The symmetry properties of a given nanotube fragment are determined by the number of hexagons along the tube axis, N , being even or odd and the number of hexagons along the tube circumference, n , being even or odd, from literature we find the structural unit of the tube is the distorted carbon hexagon [32].

For odd number of ring layers:

ρ (outer carbon atom -C) (Mono- layer) (-0.165) > ρ (outer carbon atom -C) (Tri- layer) (-0.133)

ρ (inner carbon atom -C) (Mono- layer) (-0.003) < ρ (inner carbon atom -C) (Tri- layer) (-0.037)

For even number of ring layers:

ρ (outer carbon atom -C) (Di-layer) (-0.141) < ρ (outer carbon atom -C) (Tetra- layer) (-0.190)

For even layer:

ρ (inner carbon atom -C) (Di-layer) (-0.002) < ρ (inner carbon atom -C) (Tetra- layer) (-0.003)

Tetra-layer zigzag nanotube is more semiconductor than Di-layer zigzag nanotube.

For whole correlation:

$\rho(\text{Tetra-layer}) > \rho(\text{Mono-layer}) > \rho(\text{Di-layer}) > \rho(\text{Tri-layer})$

Mono-ring layer D_{6h}		Di- ring layers D_{6d}		Tri-ring layers D_{6h}		Tetra-ring layers D_{6d}		
Electronic charge density -0.168- (+0.168)		Electronic charge density -0.158- (+0.158)		Electronic charge density -0.158-- (+0.158)		Electronic charge density -0.190- (+0.190)		
—H	0.168		—H	0.158		—H	0.158	
---C	-0.165		---C	-0.141		---C	-0.133	
	-0.003		---C	-0.014		---C	-0.041	
			---C	-0.002		---C	0.053	
						---C	-0.037	
						---C	-0.025	
						---C	-0.003	

Figure 7- Distribution of charge density at the atoms for (Mono, Di, Tri and Tetra) rings layer of (6,0) Zigzag SWCNT.

- 6- For all the polyaromatic hydrocarbons (PAHs) naphthalene, anthracene, and tetracene, the frontier molecule orbital density distributions are located mainly at the circumferential bonds as well as the carbon nanotubes [30,31]., Figure 8., and this agrees with the favorable positions of electrophilic and nucleophilic active sites [32].

Hamada et al. [33] explained that the HOMO-LUMO energy gap $\Delta E_{\text{HOMO-LUMO}}$ decreases with increasing tube fragment size of SWCNTs and this agrees with our work. Accordingly increasing the fragment size reduces the energy gap. However, changes in the HOMO-LUMO gap diminish quickly

with increasing fragment size and become negligible. Also the HOMO structure of (n,0) nanotube fragments depend on the symmetry of the fragment.

The LUMO and HOMO of these nanotube fragments are energetically degenerated and belong to the irreducible representation e_3 . In other words, the HOMO of these nanotube fragments is half-occupied. The explored LUMO and HOMO, as well as their orbitals in D_{6h} nanotube fragments, consist mainly of 2p AOs of the edge atoms. By virtue of the symmetry operations of the point group D_{6d} , such orbitals have to be doubly degenerated. The total number of electrons in the system is not sufficient to fill this orbital completely. The unpaired spins result in a net dipole moment and prevent the self-consistent calculation from converging. However, adding two extra electrons to the system (intercalation) results in zero net dipole moment for the completely filled HOMO, and the self-consistent computation converges.

From this consideration we can conclude that the charge-neutral nanotube fragments of D_{6d} symmetry are unstable. We would, however, expect a stabilization of this system by a symmetry-lowering Jahn-Teller distortion. The structures of the HOMO and LUMO orbitals in nanotube fragments of D_{6d} symmetry appear to be similar to those of D_{6h} nanotube fragments.

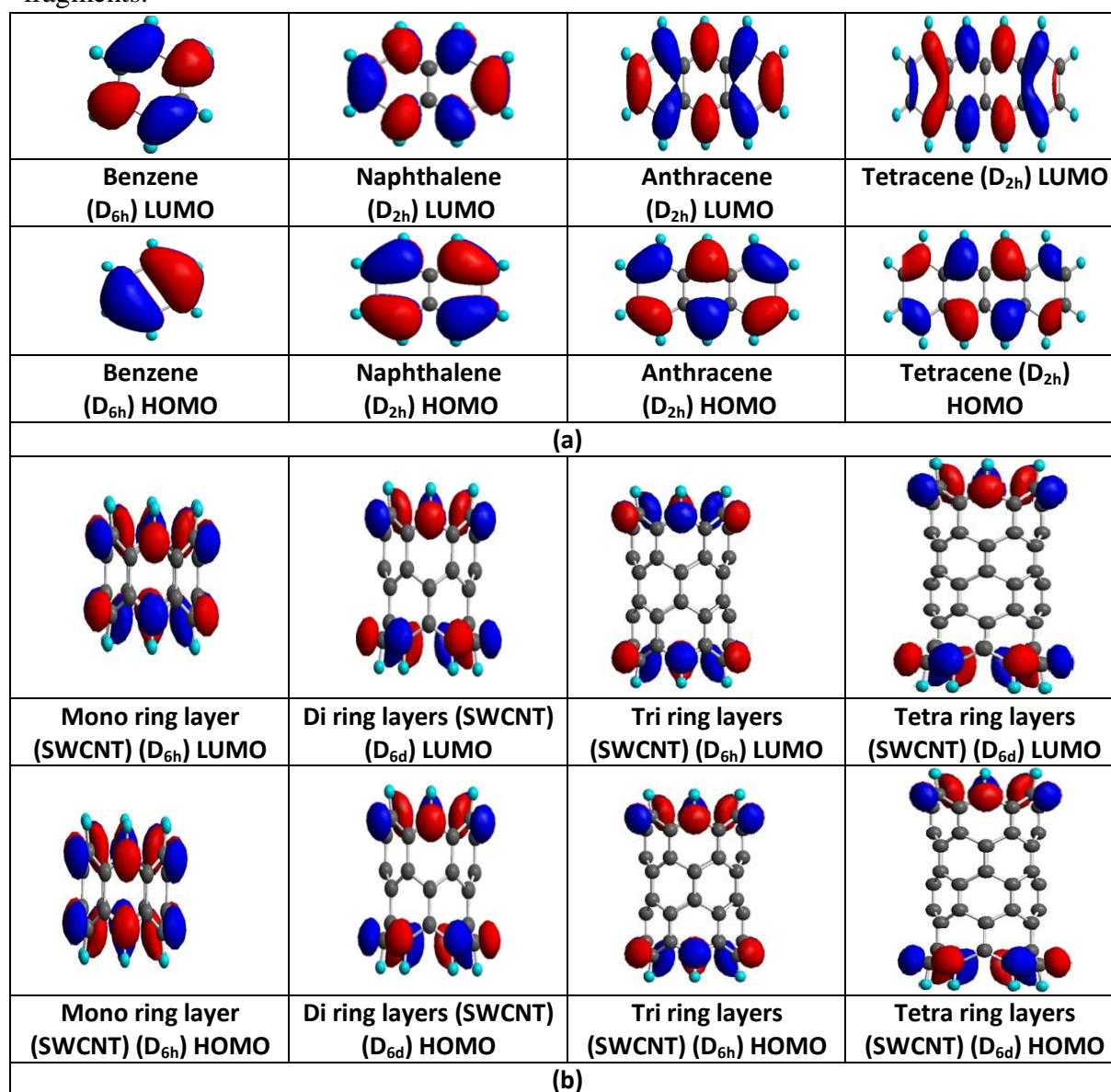


Figure 8- The frontier molecule orbital density distributions, HOMO; LUMO; (a) for benzene, naphthalene, anthracene and tetracene, (b) for Mono, Di, Tri and Tetra-rings layer (6, 0) Zigzag SWCNT.

Correlation of vibration frequencies for (6,0) zigzag SWCNTs construction units.

1. The vibration frequencies of CH stretching was found to be increased with increasing the number of ring layers for (6,0) zigzag SWCNTs, Figure-9 and Table-3.

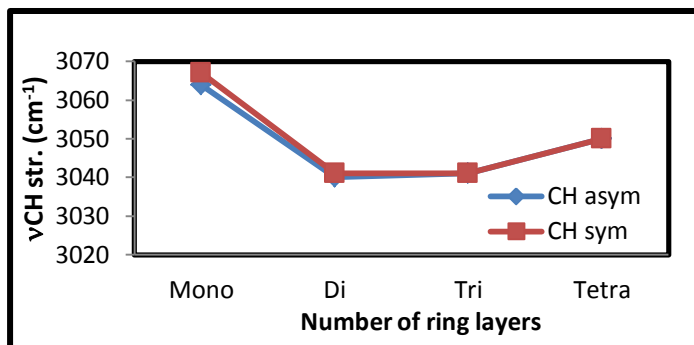


Figure 9- Correlation between the vibration frequencies of C-H stretching and the number of ring layers as calculated by DFT method.

2. The C-Cc stretching vibration frequencies increase with increasing the number of ring layers, Table-3.
3. The C-Ca stretching vibration frequencies increase (increase in force constant) for both symmetric and asymmetric vibration with increasing the number of ring layers for zigzag SWCNTs, Figure-10 and Table-3.

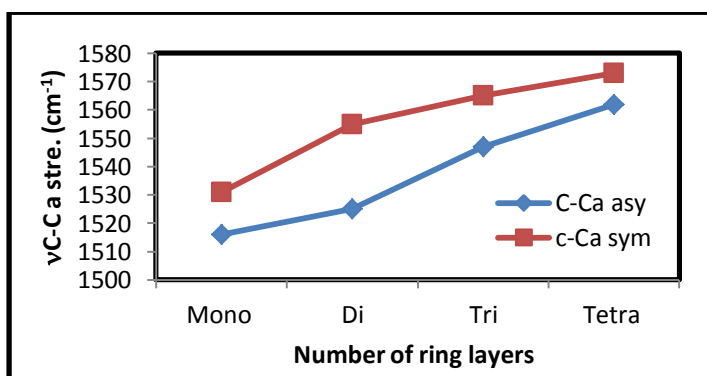


Figure 10- Correlation between the vibration frequencies of C-Ca stretching and the number of ring layers as calculated by DFT method.

4. The C-Cc stretching vibration frequencies decrease (decrease in force constant) with increasing the odd number of ring layers, and equal in value for the even number of ring layers Di and tetra zigzag SWCNT, Figure-11 and Table-3.

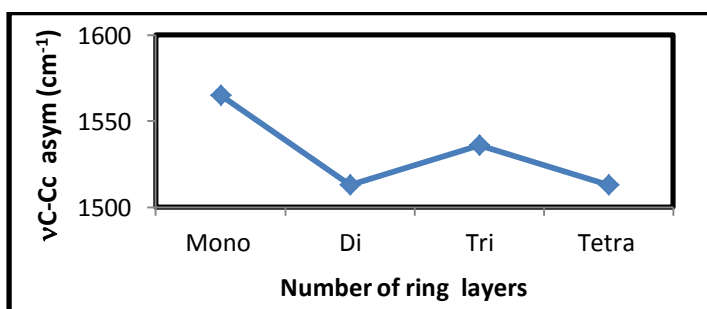


Figure 11- Correlation between the stretching vibration frequencies of C-Cc and the number of ring layers as calculated by DFT method.

5. The vibration frequencies of in plane C-H deformation (δ CH (scissoring and rocking)) for odd number ring layers decrease with increasing in the number of ring layers, and equal in value for the even number of ring layers Di and tetra zigzag SWCNT, Figure-12 and Table-3.

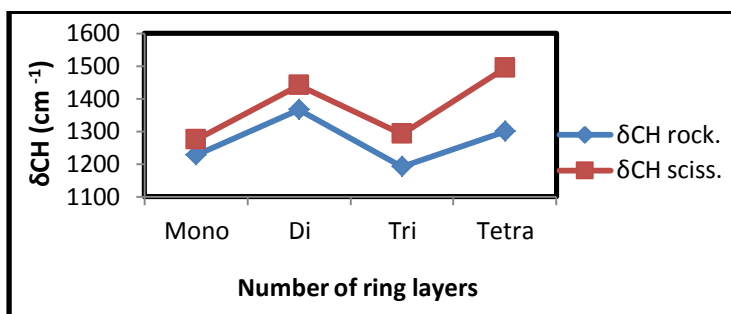


Figure 12- Correlation between the vibration frequencies of (δ CH) and the number of ring layers as calculated by DFT method.

6. The vibration frequencies of in plane ring deformation (δ ring) (increase for odd and decrease for even ring layers) with increasing number of ring layers, Figure-13 and Table-3.

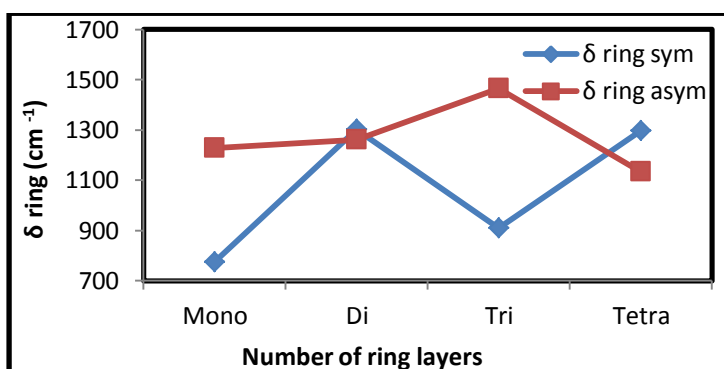


Figure 13- Correlation between the vibration frequencies of ring in plane deformation (δ ring) and the number of ring layers as calculated by DFT method.

7. The vibration frequencies of out of plane CH deformation (γ CH), decrease with increasing (odd & even) ring layers, Figure-14 and Table-3.

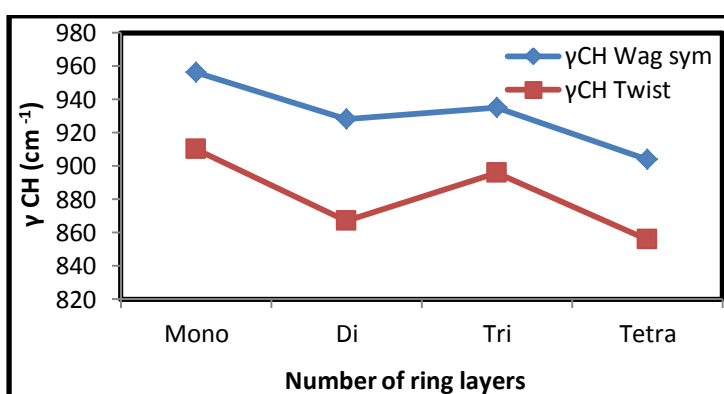


Figure 14- Correlation between the out of plane C-H deformation (γ CH) and the number of ring layers as calculated by DFT.

8. The asymmetric vibration frequencies of out of plane ring deformation (γ ring or γ CCC), decrease with increasing number of (odd & even SWCNTs), the same was shown for the symmetric vibration frequencies of even ring layers, and the reverse was shown for the symmetric (γ ring) of odd number of ring layers which increase with increasing number of ring layers Figure-15 and Table-3.

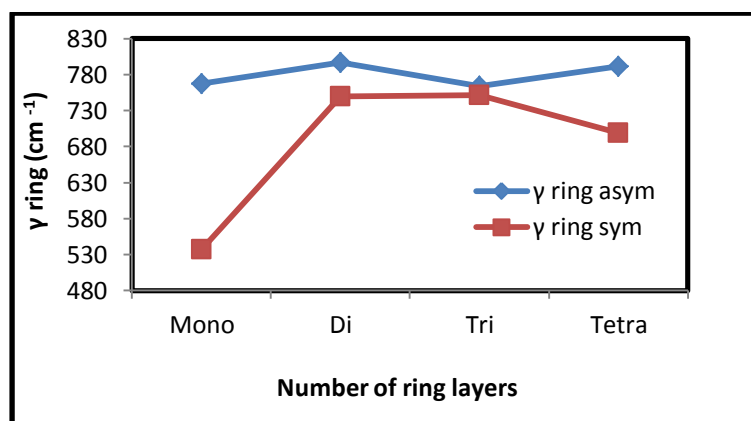


Figure 15- Correlation between number of layers and vibration of deformation ring out of plane (γ ring) as calculated by DFT.

In comparison with the frequencies of naphthalene and anthracene molecules, as calculated applying similar DFT method and gauss basis, the frequency values of (Mono, Di, Tri, Tetra) ring layers SWCNTs are lower. The comparison shows that the molecular force fields for SWCNTs are weaker than those of the coplanar polyaromatic molecules. It indicates that the influence of folding in diminishing the C-C bond strength of the aromatic molecules too, Table-3. The result parallels to that of Turker [34] who showed, on the basis of the Hückel treatment, that the electronic binding energy of the planar polyaromatic are bigger in value than those of the SWCNTs with similar number of benzene rings.

Table 3- Vibration frequencies (cm^{-1}) for some modes of construction units (6,0) zigzag SWCNTs.

Zigzag ring layer	C-H asym	C-H sym.	C-Ca asym	C-Ca sym.	C-Cc asym	$\delta\text{C-H}$ sciss.	δCH rock.	δring asym	δring sym	γCH wagg.asym	γCH wagg.sym
Naphthalene	3077 B_{2u}	3079 A_g	-----	1657 A_g	-----	1320 B_{1u}	1311 B_{3g}	1053 B_{2u}	1068 A_g	1043 B_{3u}	-----
Anthracene [30]	3066 B_{2u}	3066 A_g	-----	1592 A_g	-----	1191 B_{1u}	-----	1134 B_{3g}	767 A_g	-----	-----
Mono ring layer [35]	3064 A_{2u}	3067 A_{1g}	1516 E_{1u}	1531 A_{1g}	1565 E_{1g}	1274 B_{2g}	1227 A_{2g}	1228 E_{2u}	775 A_{1g}	936 A_{2u}	956 A_{1g}
Di ring layers	3040 B_2	3041 A_1	1525 E_1	1555 A_1	1513 E_5	1440 E_3	1367 E_1	1262 E_1	1302 A_1	931 B_2	928 A_1
Tri ring layers [36]	3041 A_{2u}	3041 A_{1g}	1547 E_{1u}	1565 A_{1g}	1536 E_{1g}	1291 E_{1u}	1191 E_{1u}	1466 E_{2u}	911 E_{2g}	899 E_{1u}	935 A_{1g}
Tetra ring layers	3050 B_2	3050 A_1	1562 B_2	1573 A_1	1513 E_5	1494 E_4	1300 E_1	1135 E_4	1297 A_1	893 B_2	904 A_1

Table 3. shows the following relations.

- The C-H_{asym} vibrations decrease with increasing number of odd rings layer, and increase with increasing number of even rings layer.
- The C-H_{sym} vibrations decrease with increasing number of odd rings layer, and increase with increasing number of even rings layer.
- The C-Ca_{asym} vibrations increase with increasing number of odd rings layer, and number of even rings layer.
- The C-Ca_{sym} vibrations increase with increasing number of odd rings layer, and number of even rings layer.
- The C-Cc_{asym} vibrations decrease with increasing number of odd rings layer, and equal in even number of rings layer.
- The δ CH scissoring vibrations increase with increasing number of odd rings layer, and even number of rings layer.
- The δ CH rocking vibrations decrease with increasing number of odd rings layer, and even number of rings layer.
- The δ ring_{asym} vibrations increase with increasing number of odd number of rings layer, and decrease with increase of even number of rings layer.
- The δ ring_{sym} vibrations increase with increasing number of odd rings layer, and decrease with increase of even number of rings layer.
- γ CH_{asym} wagging vibrations decrease with increasing number of odd rings layer, and even number of rings layer.
- γ CH_{sym} wagging vibrations decrease with increasing number of odd number of rings layer, and even number of rings layer.
- γ CH twisting vibrations decrease with increasing number of odd rings layer, and even number of rings layer.
- γ ring_{asym} vibrations decrease with increasing number of odd rings layer, and even number of rings layer.
- γ ring_{sym} vibrations increase with increasing number of odd rings layer, and decrease with increasing even number of rings layer.

Decreasing the vibrational motions of atoms increase the electrical conductivity properties [26-31]. This agrees with vibrational frequencies found for odd (6,0) zigzag SWCNTs (Mono & Tri) SWCNTs. SWCNTs (6,0) zigzag with even number of ring layers (Di & Tetra) were found to be unstable in their singlet state (show some imaginary vibrational frequencies), they are stable at triplet state [37]. For this reason the vibrational motion increased with increased number of even ring layers.

Conclusions

- Different relations result from the research of the construction units of (6,0) zigzag SWCNTs. These results include the internal coordinates i.e "bonds length and angles", accompanied with some energetic and physical properties such as standard heat of formation ΔH°_f , dipole moment μ , energy of high occupied molecular orbital E_{HOMO} , energy of low unoccupied molecular orbital E_{LUMO} , $\Delta E_{HOMO-LUMO}$, vibration frequencies, infra-red (IR) absorption intensities, and distribution of electronic charge for different symmetries. These molecules have different symmetries and stabilization energies, with physical and conductivity properties which accompanied these symmetries that are applied for the industrial purposes.
- Vibrational motion of atoms decreases the electrical conductivity of nanotubes and limits the performance of nano transistors and other electronic devices based on them.
- Nanotubes possess extraordinary mechanical properties and are among the strongest materials known.

- Based on the direction distribution of electronic charge results, the electronic charge is concentrated at the edge of tube and the outer atoms of molecules. These results are in a good with other scientific researches.
- Charge densities concentrated at hydrogen atoms (positively charged) and at the outer circumferential carbon atoms (negatively charge).
- Axial carbon atoms have diminishing charges from outer to the center of the CNTs.
- $\Delta E_{\text{HOMO-LUMO}}$ was found to be decreased with increasing ring layers of SWCNTs leading to better physical property of electronic conductivity.

References

1. Wang, Q.H. Setlur, A.A. Lauerhaas, J.M. Dai, J.Y. Seelig, E.W. and Chang, R.P.H. **1998**. A nanotube-based field-emission flat panel display, *Appl. Phys. Lett.* 72, pp: 2912-2913.
2. Treacy, M.M.J. Ebbesen, T.W. and Gibson, J.M. **1996**. Exceptionally high Young's modulus observed for individual carbon nanotubes, *Nature*, 381, pp: 678–680.
3. a-Wong, E.W. Sheehan, P.E. Lieber, C.M. **1997**. Nanobeam Mechanics: Elasticity, Strength, and Toughness of Nanorods and Nanotubes., *Science*, 277 (5334), pp: 1971–1975., b- Choudhary N, Hwang S, Choi W. **2014**. *Carbon nanomaterials: a review. In Handbook of Nanomaterials Properties, USA: Springer;* p. 709., c- Osman, M. Cummings, A. and Srivastava, D. **2007**. Thermal Properties of Carbon Nanotubes, *Molecular Building Blocks for Nanotechnology*. 109, pp: 154-187.
4. Eatemadi1, A. Daraee1, H. Karimkhanloo1, H. Kouhi4 M. Zarghami1, N. Akbarzadeh, A. Abasi1, M. Hanifehpour, Y. and Joo, S.W. **2014**. Carbon nanotubes: properties, synthesis, purification, and medical applications Nanoscale., *Nanoscale Research Letters*, 9(393), pp: 1-13.
5. Chang, Q.S. **2009**. Thermo-mechanical behavior of low-dimensional systems: The local bond average approach., *Progress in Materials Science*; 54, pp: 179–307.
6. Moniruzzaman, M. Sahin, A. and Winey, K.I. **2009**. Improved mechanical strength and electrical conductivity of organogels containing carbon nanotubes, *CARBON*, 47, pp: 645–650.
7. Lolli, G. Zhang, L. A. Balzano, L. Sakulchaicharoen, N. Tan, Y. Q. and Resasco, D.E. **2006**, Tailoring (n,m) structure of single-walled carbon nanotubes by modifying reaction conditions and the nature of the support of CoMo catalysts, *J. Phys. Chem. B*(110), pp: 2108-2115.
8. Obot, I.B. Egbedi, N.O and Umoren, S.A. **2009**. Adsorption characteristics and corrosion inhibitive properties of clotrimazole for Aluminium corrosion in hydrochloric acid., *Int. J. Electro. chem. Sci.* 4, pp: 863-877.
9. Betune, D.S. Kiang, C.H. de Vries, M.S. Gorman, G. Savoy, R. Vazquez, J. and R. Bevers, **1993** . Cobalt-Canalized Growth of Carbon Nanotubes with Single-layer Walls, *Nature*, 363, pp: 605-607.
10. Kokai, F. Takahashi, K. Yudasaka, M. Yamada, R. Ichihashi, T. and Iijima, S. **1999**. Growth Dynamics of Single-wall Carbon Nanotubes Synthesized by 2 CO Laser Vaporization, *J. Phys. Chem.* 103(21), pp: 4346–4351.
11. Krishan, A. Dujardin, E. Ebbesen, T.W. Yianilos, P.N. and Treacy, M.M.J. **1998**. Young's modulus of single-walled nanotubes, *Phys. Rev. B*(58), pp: 14013-14019.
12. Poncharal, P. Wang, Z.L. Ugarte, D. and Deheer, W.A. **1999**. Electrostatic deflection and electromechanical resonators, *Science*, 283, pp: 1513-1516.
13. a- Zhao, Q. Gan, Z.H. and Zhuabg, O.K. **2002**. Electrochemical sensors based on carbon nanotubes, *Electroanalysis, Electroanal.*, 14, pp. 1609., b- Zhang, Y.Y. Wang, C.M. and Tan, V.B.C. **2009**. Assessment of Timoshenko Beam Models for Vibrational Behavior of Single-Walled Carbon Nanotubes using Molecular Dynamics, *Adv. Appl. Math. Mech.*, 1(1), pp: 89-106 .
14. Yao, N. and Lordi, V. **1998**. Young's modulus of single-walled carbon nanotubes, *J. Appl. Phys.* 84, pp: 1939-1943.
15. Yakobson, B.I. Brabec, C.J. and Bernholc, J. **1996**. Nanomechanics of carbon tubes: Instabilities beyond linear response, *Phys. Rev. Lett.* 76, pp: 2511-2514.
16. Buehler, M.J. Kong, J. and Gao, H.J. **2004**. Deformation mechanism of very long single-wall carbon nanotubes subject to compressive loading, *Journal of Engineering Materials and Technology*. 126, pp: 245-249.

17. Yakobson, B.I. Campbell, M.P. Brabec, C.J. and Bernholc, J. **1997**. High strain rate fracture and C-chain unraveling in carbon nanotubes, *Comp. Mater. Sci.* 8, pp: 341-348.
18. Burghard M. **2005**. Electronic and vibrational properties of chemically modified single-wall carbon nanotubes. *Surface Science Reports*, 58, pp: 1–109.
19. Zhang, Y.Y. Tan, V.B.C. and Wang, C.M. **2006**. Effect of chirality on buckling behavior of single-walled carbon nanotubes, *J. Appl. Phys.*, 100, pp: 074304-074310.
20. Zhang, Y.Y. Tan, V.B.C. and Wang, C.M. **2007**. Effect of strain rate on the buckling behavior of single- and double-walled carbon nanotubes, *Carbon*, 45, pp: 514-523.
21. Lucas, A.A. Lambin, P.H. and Smalley, R.E. **1993**. On the energetics of tubular fullerenes, *J. Phys. Chem.Solids*, 54, pp: 587-593.
22. Sawada, S. and Hamada, N. **1992**. Energetics of carbon nano-tubes, *Solid State Commun*, 83(11), pp: 917-919.
23. Frisch, M.J. Trucks, G.W. Schlegel, H.B. Scuseria, G.E. Robb, M.A. Cheeseman, J.R. Montgomery, J.A. Jr., Vreven, T. Kudin, K.N. Burant, J.C. Millam, J.M. Iyengar, S.S. Tomasi, J. Barone, V. Mennucci, B. Cossi, M. Scalmani, G. Rega, N. Petersson, G.A. Nakatsuji, H. Hada, M. Ehara, M. Toyota, K. Fukuda, R. Hasegawa, J. Ishida, M. Nakajima, T. Honda, Y. Kitao, O. Nakai, H. Klene, M. Li, X. Knox, J.E. Hratchian, H.P. Cross, J.B. Bakken, V. Adamo, C. Jaramillo, J. Gomperts, R. Stratmann, R. E. Yazyev, O. Austin, A.J. Cammi, R. Pomelli, C. Ochterski, J.W. Ayala, P.Y. Morokuma, K. Voth, G.A. Salvador, P. Dannenberg, J.J. Zakrzewski, V.G. Dapprich, S. Daniels, A.D. Strain, M.C. Farkas, O. Malick, D.K. Rabuck, A. D. Raghavachari, K. Foresman, J. B. Ortiz, J. V Cui, Q. Baboul, A. G. Clifford, S. Cioslowski, J. Stefanov, B.B. Liu, G. Liashenko, A. Piskorz, P. Komaromi, I. Martin, R.L. Fox, D.J. Keith, T. Al-Laham, M.A. Peng, C.Y. Nanayakkara, A. Challacombe, M. Gill, P.M. W. Johnson B. Chen, W. Wong, M.W. Gonzalez, C. and Pople, J.A. **2003**. *Gaussian 03*, Gaussian. Inc. Pittsburgh PA.
24. Becke A.D. **1993**. Density-functional thermochemistry. III. The role of exact exchange, *Chem. Phys.* 98, pp: 5648-5652.
25. Lee, C. Yang, W. and Parr, R.G **1988**. Development of the Colle-Salvetti correlation energy formula into a functional of the electron density, *Phys. Rev. B*(41), pp: 785-789.
26. Budyka, M.F. Zyubina, T.S. Ryabenko, A.G. Lin, S.H. Mebel, A.M. **2005**. Bond lengths and diameters of armchair single wall carbon nanotubes, *Chemical Physics Letters*, 407, pp: 266–271.
27. Gece, G. **2008**. The use of quantum chemical methods in corrosion inhibitor studies, *Corros. Sci.* 50, pp: 2981-2992.
28. Krcmar, M. Saslow, W.M. and Zangwill, A. **2003**. Electrostatic of Conducting Nanocylinder, *J. Appl. phys.* 93, pp: 3495-3500.
29. Odom, T.W. Huang, J. Kim, P. and Lieber, C.M. **2000**. Structure and Electronic Properties of CNT, *J. Phy. Chem.* 104, pp: 2794-2809.
30. a- Kubba, R.M. AL-Ani, H.N., and Shanshal M., **2011**. The Vibration Frequencies of [6] Cyclacenes (Linear, Angular and Angular-Chiral) Monoring Molecules, *Jordan journal of chemistry*, 6(3), pp: 269-290., b- Kubba, R.M. and AL-Ani, H.N. **2013**. Comparison study of CC and CH Vibration frequencies and electronic properties of mono, Di, Tri, and Tetra-rings layer of Arm chair (SWCNTs), *Iraqi journal of Physics*, 11(20), PP: 85-99.
31. Bulusheva, L.G. Okotrub, A.V. Romanov, D.A. and Tomanek, D. **1998**. Electronic Structure of (n,0) Zigzag Carbon Nanotubes: Cluster and Crystal Approach, *J. Phys. Chem. A*(102), pp: 975-981.
32. Fleming, I. **1976**. *Frontier Orbitals and Organic Chemical Reactions*. Ed¹, John Wiley and Sons, NewYork.
33. Hamada, N. Sawada, S. and Oshiyama, A. **1992**. New one-dimensional conductors: graphitic microtubules, *Phys. Rev. Lett.* 68(10), pp: 1579–1581.
34. Turker, L. **2000**. The Effect of Peripheral Circuits on the Total p-Electron Energies of Cyclacenes, *Turk. J. Chem.* 24, pp: 217-222.
35. Kubba, R.M. AL-Ani, H.N., and Shanshal M., **2011**. Calculated Vibration Frequencies and IR Absorption Intensities of [6] Cyclacene (zig zag) Molecule, *American Journal of Scientific and Industrial Research (AJSIR)*, 2, pp: 642-651.

36. Kubba, R.M. and Samawi, K.A. **2014**. Theoretical Study of Electronic Properties and Vibration Frequencies for Tri-Rings Layer (6,0) Linear (Zigzag) SWCNT, *Iraqi Journal of Science*, 55(2B), pp: 606-616.
37. Samawi, K.A. **2014**. Comparison Study of Physical Properties and Energies for Construction Units of Fullerene Molecule and for (ZigZag) SWCNTs Using Quantum Mechanical Methods, Ph.D. *Thesis*, Department of chemistry, College of Science, University of Baghdad, Jadiriya, Baghdad, Iraq.